CD44 is a determinant of inflammatory bone loss

Silvia Hayer,[1,3] Günter Steiner,[1,3,4] Birgit Görtz,[3] Erika Reiter,[1] Makiyeh Tohidast-Akrad,[4] Michael Amling,[5] Oskar Hoffmann,[2] Kurt Redlich,[1] Jochen Zwerina,[1] Karl Skriner,[1] Frank Hilberg,[6] Erwin F. Wagner,[7] Josef S. Smolen,[1,3,4] and Georg Schett[1,3]

[1]Division of Rheumatology, Department of Internal Medicine III, Medical University of Vienna, A-1090 Vienna, Austria
[2]Institute of Pharmacology and Toxicology, University of Vienna, A-1090 Vienna, Austria
[3]Center of Molecular Medicine of the Austrian Academy of Sciences (CeMM), A-1090 Vienna, Austria
[4]Ludwig Boltzmann-Institute for Rheumatology, A-1130 Vienna, Austria
[5]Department of Experimental Trauma Surgery, University School of Hamburg, D-20146 Hamburg, Germany
[6]Boehringer Ingelheim, A-1121 Vienna, Austria
[7]Research Institute of Molecular Pathology, A-1030 Vienna, Austria

Chronic inflammation is a major trigger of local and systemic bone loss. Disintegration of cell–matrix interaction is a prerequisite for the invasion of inflammatory tissue into bone. CD44 is a type I transmembrane glycoprotein that connects a variety of extracellular matrix proteins to the cell surface. Tumor necrosis factor (TNF) is a major inducer of chronic inflammation and its overexpression leads to chronic inflammatory arthritis. By generating $CD44^{-/-}$ human TNF-transgenic (hTNFtg) mice, we show that destruction of joints and progressive crippling is far more severe in hTNFtg mice lacking CD44, which also develop severe generalized osteopenia. Mutant mice exhibit an increased bone resorption due to enhanced number, size, and resorptive capacity of osteoclasts, whereas bone formation and osteoblast differentiation are not affected. Responsiveness of CD44-deficient osteoclasts toward TNF is enhanced and associated with increased activation of the p38 mitogen-activated protein kinase. These data identify CD44 as a critical inhibitor of TNF-driven joint destruction and inflammatory bone loss.

CORRESPONDENCE
Georg Schett:
georg.schett@meduniwien.ac.at

Abbreviations used: hTNFtg, human TNF-transgenic; MAPK, mitogen-activated protein kinase; micro-CT, microcomputed tomography; MKP, MAPK phosphatase; OPG, osteoprotegerin; RA, rheumatoid arthritis; RANKL, receptor activator of NF-κB ligand; TRAP, tartrate-resistant acidic phosphatase.

Chronic inflammation in combination with systemic bone loss and severe joint damage is a characteristic of rheumatoid arthritis (RA; references 1–4). Given its destructive course and the associated functional impairment, RA is a highly disabling disease (5). Recently, osteoclasts have been identified as key cell population–mediating, inflammation-triggered bone erosions (6). In fact, chronic inflammatory tissue, such as the RA synovial membrane, provides a suitable microenvironment to promote differentiation of osteoclasts (7). Once formed, these cells pave the path for invasion of inflammatory tissue into bone. Strikingly, osteoclast-deficient mice can develop arthritis, but inflammation is not accompanied by bone destruction (8, 9). The factors that regulate osteoclast formation and bone destruction in the course of chronic inflammatory processes, however, are poorly characterized.

The membrane-bound surface receptor CD44 provides a link between extracellular matrix components and the cell surface (10). CD44 comprises a family of transmembrane glycoproteins encoded by a single gene. Due to great variability in splicing, 17 different isoforms can be generated. Interestingly, $CD44^{-/-}$ mice lacking all isoforms of CD44 have no obvious phenotype (11). Nevertheless, CD44 has been shown as functionally significant in hematopoiesis, lymphocyte homing, and development of tumor metastasis. Furthermore, a major physiological role of CD44 is the maintenance of tissue homeostasis through connecting several matrix components, such as hyaluronic acid, chondroitin sulfate, and osteopontin to the cell surface (10, 12, 13). Therefore, we hypothesized that function of CD44 may gain critical importance in chronic inflammatory conditions, because resulting tissue damage and

B. Görtz's present address is Institute of Pathology, University of Giessen, 35390 Giessen, Germany.
K. Skriner's present address is Rheumatology & Clinical Immunology, Charité, D-10117 Berlin, Germany.

bone destruction require disintegration of normal cell–matrix interactions. To address this hypothesis, we crossed CD44$^{-/-}$ mice with human TNF-transgenic (hTNFtg) mice (14), which develop a chronic inflammatory arthritis followed by joint destruction and osteopenia closely resembling human RA. The resulting CD44$^{-/-}$ hTNFtg mice develop a very aggressive form of arthritis, which is more severe than in hTNFtg animals. This phenotype is characterized by increased formation of articular osteoclasts, which are increased in number and size both in vitro and in vivo. In addition, loss of CD44 enhances systemic bone loss induced by TNF overexpression. These results suggest that CD44 functions as an inhibitor of inflammatory bone loss.

RESULTS

Generation and phenotypic characterization of CD44$^{-/-}$ hTNFtg mice

To investigate the role of cell–extracellular matrix interaction in inflammatory bone destruction, hTNFtg mice were crossed with CD44$^{-/-}$ mice. The offspring of all four genotypes (WT, CD44$^{-/-}$, hTNFtg, and CD44$^{-/-}$ hTNFtg) were born in Mendelian frequency and were viable and phenotypically indistinguishable at birth. As described, CD44$^{-/-}$ mice developed no obvious phenotype during the entire observation period (up to week 10) and showed no difference in size and body weight compared with WT mice. In contrast, the two genotypes carrying the TNF transgene (hTNFtg and CD44$^{-/-}$ hTNFtg) developed clinical signs of arthritis at the age of 4 wk. In addition, they showed a marked and significant reduction of >20% in body weight.

Clinical investigation revealed progressive joint swelling in both hTNFtg and CD44$^{-/-}$ hTNFtg mice (Fig. 1 A), but in the latter, disease activity was significantly enhanced and progressed significantly faster (Fig. 1 B; $P < 0.01$), whereas no articular changes were found in WT and CD44$^{-/-}$ mice. In addition, grip strength of paws deteriorated significantly faster in CD44$^{-/-}$ hTNFtg mice, suggesting rapid loss of joint

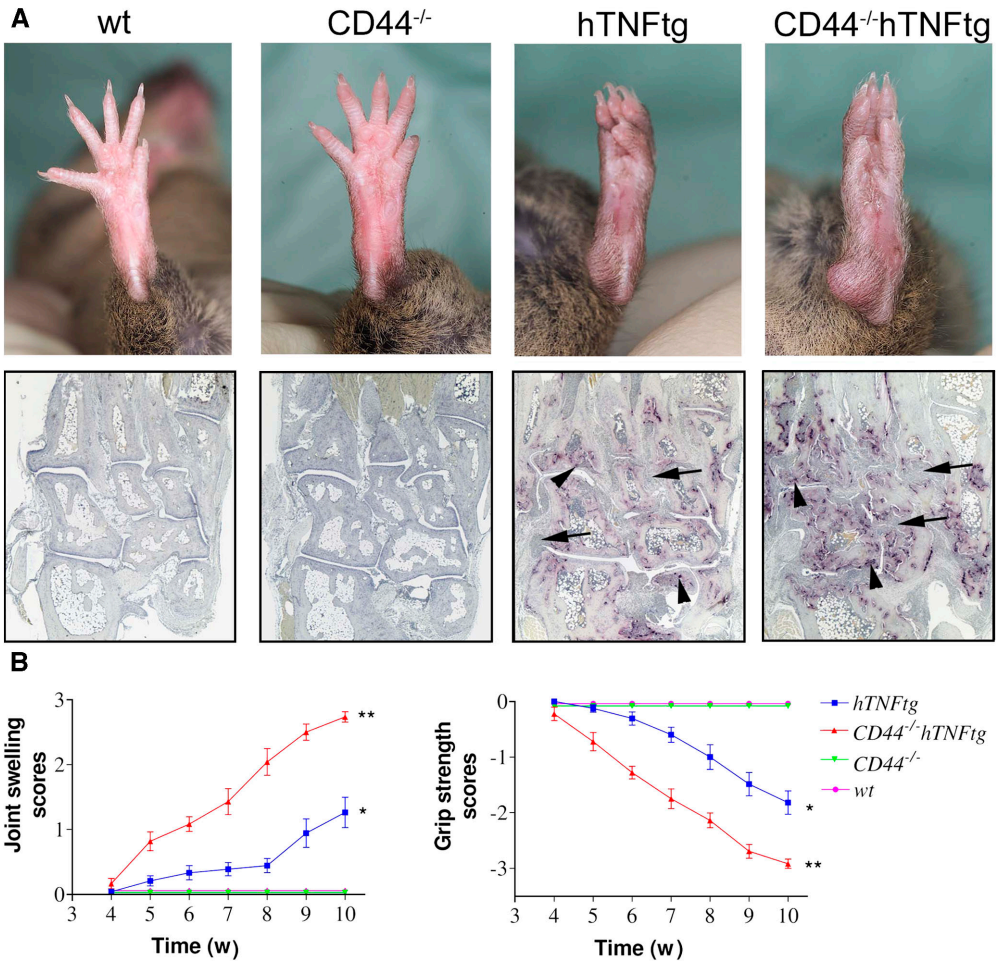

Figure 1. Clinical signs of arthritis. (A) WT (wt) and CD44$^{-/-}$ mice (aged 10 wk) showed normal hind paws, hTNFtg mice developed paw inflammation, and CD44$^{-/-}$ hTNFtg showed severe inflammation and deformities of paws. Histology (TRAP stain; original magnification of 250) of the same paws showing inflammation (arrows) and bone destruction (arrowheads; purple spots). (B) Clinical course of paw swelling and loss of grip strength between 4 and 10 wk of age.

function (Fig. 1 B). These changes were the consequence of severe synovitis with increased numbers of osteoclasts, resulting in destruction of the normal joint architecture.

Increased joint destruction and enhanced numbers of osteoclasts in the absence of CD44

Next, we performed a detailed histological analysis of joints in the front and hind paws. Inflammatory bone erosions were significantly increased in CD44$^{-/-}$ hTNFtg mice compared with hTNFtg mice. Osteoclasts were abundant at the interface of inflammatory synovial tissue and bone (Fig. 2 B). Quantitative analyses revealed significantly larger areas of erosions and increased numbers of osteoclasts in CD44$^{-/-}$ hTNFtg mice compared with hTNFtg controls (Fig. 2 A), suggesting increased generation and activity of osteoclasts in inflammatory tissue of CD44$^{-/-}$ hTNFtg mice. Moreover, the osteoclasts of CD44$^{-/-}$ hTNFtg mice appeared to be much larger in size than those of hTNFtg animals. In addition, cartilage damage was increased in CD44$^{-/-}$ hTNFtg mice, as denoted by widespread loss of proteoglycans in the articular cartilage (Fig. 2 C). Immunohistochemical analyses revealed significant CD44 expression in osteoclast-rich areas at the interface of inflammatory tissue and bone in hTNFtg mice, whereas it was completely absent in CD44$^{-/-}$ hTNFtg mice (Fig. 2 D). Nevertheless, CD44$^{-/-}$ hTNFtg animals had similar expression patterns of CD44 ligands, such as hyaluronic acid (Fig. 2 E) or osteopontin (not depicted).

Severe systemic osteopenia in CD44$^{-/-}$ hTNFtg mice is due to enhanced bone resorption

Next, we investigated whether bone was also affected at sites distant from inflammatory tissue. Of note, hTNFtg mice resemble a model of inflammation-triggered generalized bone loss (15). Histological analysis of the axial and peripheral skeleton revealed similar bone mass and structure in WT and CD44$^{-/-}$ mice (Fig. 3 A). In contrast, hTNFtg mice exhibited bone loss in both the axial and peripheral skeletal compartment, which was significantly aggravated in CD44$^{-/-}$ hTNFtg mice (Fig. 3 A). Microcomputed tomography (micro-CT) analysis revealed that low bone mass in CD44$^{-/-}$ hTNFtg mice was due to a decrease of trabecular structures as well as thinning of cortical bone (Fig. 3, B and C).

To address the bone phenotype of CD44$^{-/-}$ hTNFtg mice in more detail, we analyzed bones of all four genotypes by histomorphometry. Trabecular bone volume was comparable in WT and CD44$^{-/-}$ mice. hTNFtg mice showed a significantly lower trabecular bone volume, which further decreased in CD44$^{-/-}$ hTNFtg mice (Fig. 4, A and B). These differences were based on the low numbers of trabeculae among CD44$^{-/-}$ hTNFtg mice as well as decreased tra-

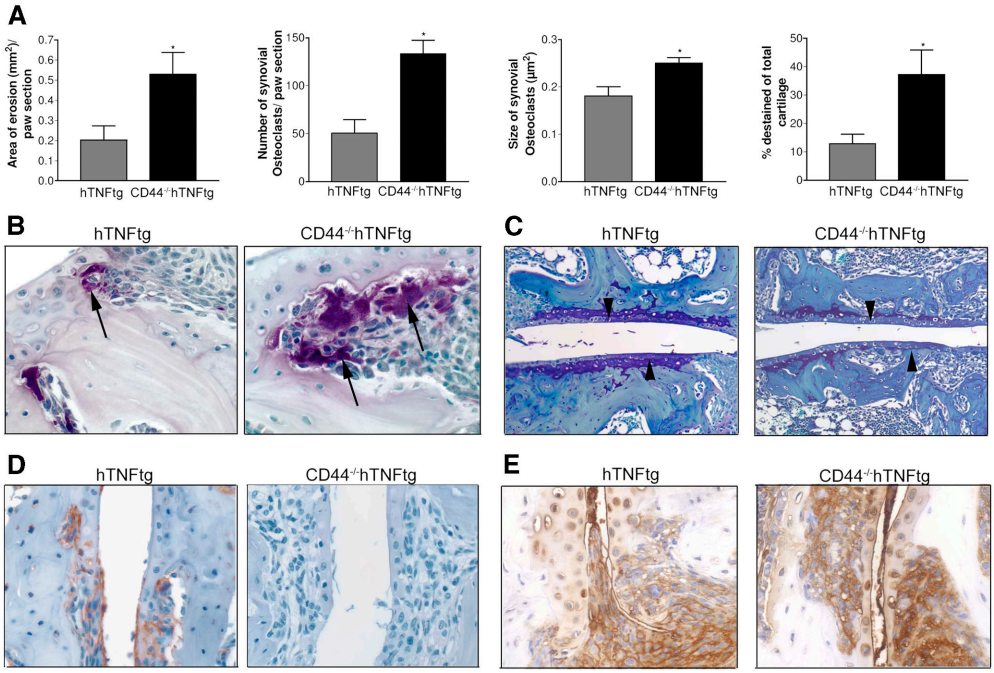

Figure 2. Histological analysis of arthritis. (A) Quantitative morphometric analysis of bone erosion, numbers, and size of synovial osteoclasts and cartilage proteoglycan loss. Data are expressed as mean ± SD. Asterisks indicate significant ($P < 0.05$) difference between hTNFtg and CD44$^{-/-}$ hTNFtg mice. (B) TRAP stain showing osteoclasts (purple, arrows) in inflammatory bone erosions of hTNFtg and CD44$^{-/-}$ hTNFtg mice. (C) Toluidine blue stain indicating cartilage damage due to loss of proteoglycans (destained areas, arrowheads). (D) Immunohistochemistry showing expression of CD44 (brown). (E) Detection of hyaluronic acid content in the paws of hTNFtg and CD44$^{-/-}$ hTNFtg mice by hyaluronic acid binding protein (brown). Original magnification of 100 (C) and 400 (B, D, and E).

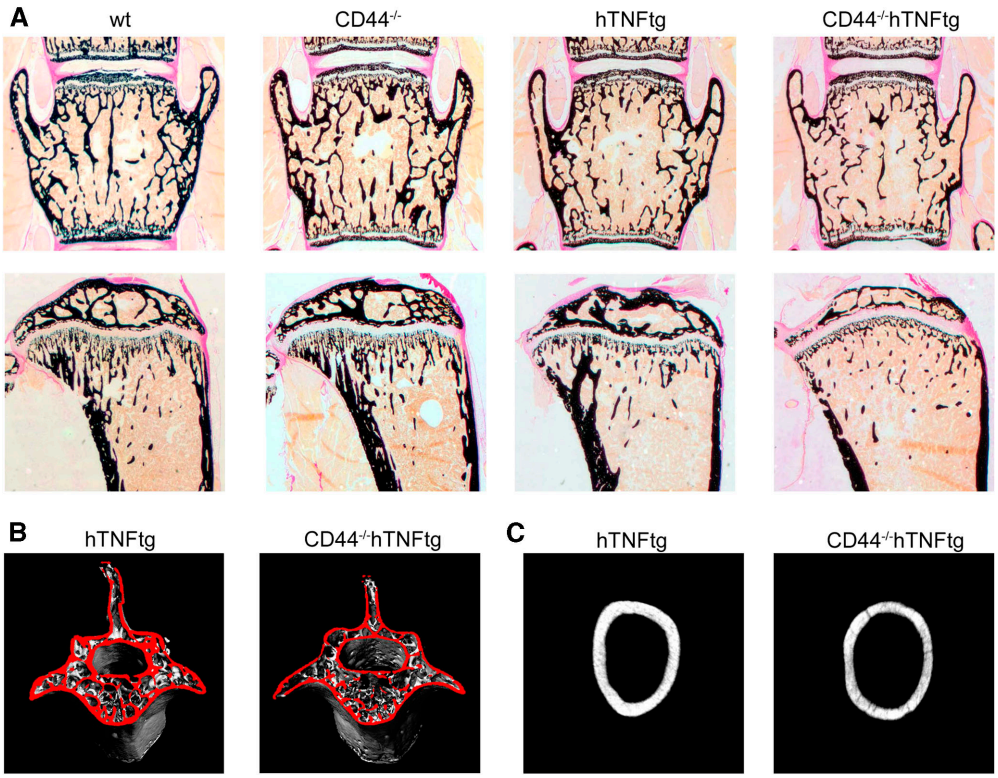

Figure 3. Histological and micro-CT analysis of systemic bone. (A) Von Kossa staining of vertebrae and tibiae from 10-wk-old WT, CD44$^{-/-}$, hTNFtg, and CD44$^{-/-}$ hTNFtg mice (original magnification of 25). (B) Micro-CT–based 3D reconstruction of vertebrae from hTNFtg and CD44$^{-/-}$ hTNFtg mice. (C) Micro-CT showing transversal sections through femoral shafts of hTNFtg and CD44$^{-/-}$ hTNFtg mice.

becular thickness. In addition, CD44$^{-/-}$ hTNFtg mice showed a massive increase in numbers of osteoclasts and osteoclast-covered surface not only compared with WT and CD44$^{-/-}$ mice (Fig. 4, A and B), but also compared with hTNFtg mice. In contrast, osteoblast numbers and osteoblast-covered surface (not depicted) were not different between hTNFtg mice and CD44$^{-/-}$ hTNFtg mice, suggesting that the low bone volume of CD44$^{-/-}$ hTNFtg mice might be due to increased bone resorption. These data were further supported by the finding that serum parameters of bone resorption (cross-laps) were highest in CD44$^{-/-}$ hTNFtg mice, whereas serum osteocalcin levels as parameter of bone formation did not differ between the two hTNFtg genotypes (Fig. 4 C).

Functional characterization of bone cells from CD44$^{-/-}$ hTNFtg mice

To characterize the functional changes of bone cells leading to the highly destructive and osteopenic phenotype of CD44$^{-/-}$ hTNFtg mice, we analyzed in vitro osteoclastogenesis and osteoblastogenesis. Upon stimulation with M-CSF and receptor activator of NF-κB ligand (RANKL), comparable amounts of tartrate-resistant acidic phosphatase (TRAP)$^{+}$ multinucleated osteoclasts were formed in cell cultures from WT and CD44$^{-/-}$ mice, whereas osteoclastogenesis was enhanced in cultures from hTNFtg mice, as described previously (16). Remarkably, osteoclastogenesis was substantially more increased in CD44$^{-/-}$ hTNFtg mice, as denoted from the formation of numerous, giant-sized osteoclasts (Fig. 5 A). In line with this finding, the analysis of the functional state of osteoclasts by measuring bone resorption pits revealed extensive areas of bone resorption in CD44$^{-/-}$ hTNFtg mice (Fig. 5 B). Enumeration showed a higher number of osteoclasts in CD44$^{-/-}$ hTNFtg mice, and these cells were bigger in size and displayed an enormously increased capacity to form resorption pits (Fig. 5 C). Time response curves revealed that osteoclasts formed earlier, more abundantly, and persisted for a longer time (Fig. 5 C). These differences were based on a higher proliferative activity of hTNFtg osteoclasts, independent of CD44, and a significantly reduced rate of apoptosis in CD44$^{-/-}$ hTNFtg cells (Fig. 5 C). CD44$^{-/-}$ hTNFtg osteoclasts showed a particularly high expression of TRAP and calcitonin receptor compared with hTNFtg osteoclasts, whereas other markers such as MMP-9 and cathepsin K were equally expressed (Fig. 5 D). On the other hand, osteoblastogenesis, as measured by the formation of cells producing alkaline phosphatase as well as bone nodule formation, was not different between hTNFtg and CD44$^{-/-}$ hTNFtg mice (not depicted).

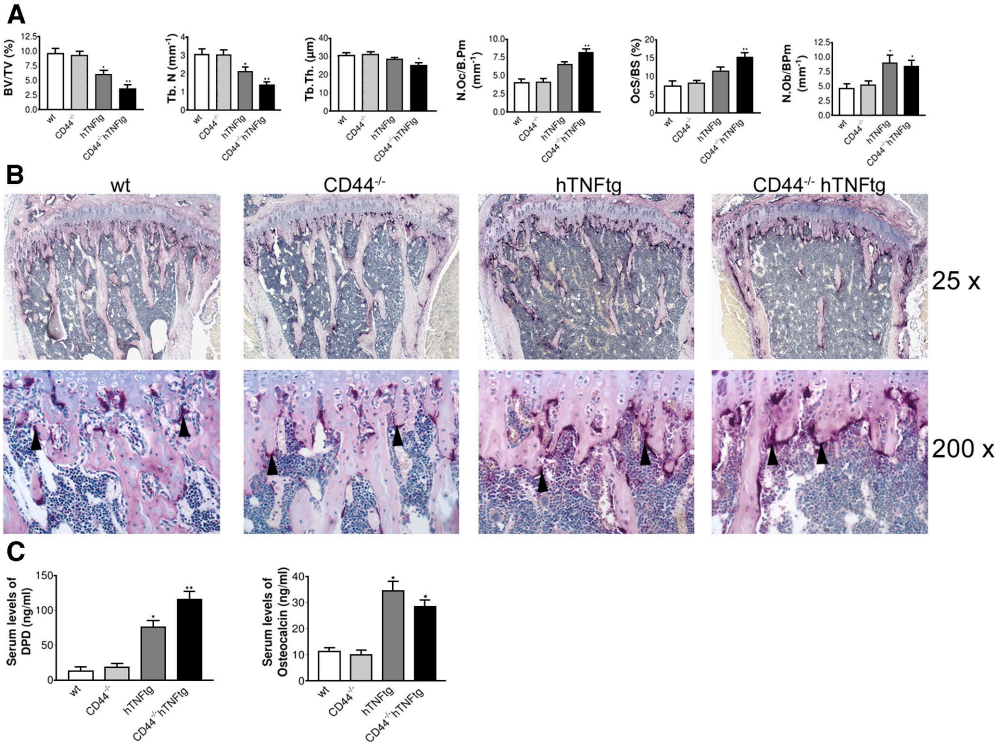

Figure 4. Histomorphometry of systemic bone. (A) Tibial metaphyses of WT, CD44$^{-/-}$, hTNFtg, and CD44$^{-/-}$ hTNFtg mice were analyzed for bone volume per tissue volume (BV/TV), trabecular number (Tb.N), trabecular thickness (Tb.Th), number of osteoclasts per bone perimeter (N.Oc/B.Pm), osteoclast surface per bone surface (OcS/BS), and the number of osteoblasts per bone perimeter (N.Ob). Data are mean ± SD. Asterisks indicate significant ($P < 0.05$) differences: *, hTNFtg and CD44$^{-/-}$ hTNFtg compared with WT and CD44$^{-/-}$; **, CD44$^{-/-}$ hTNFtg compared with hTNFtg. (B) TRAP-stained sections of tibial metaphyses from WT, CD44$^{-/-}$, hTNFtg, and CD44$^{-/-}$ hTNFtg mice show trabecular bone and osteoclasts (purple, arrowheads). Original magnification of 25 (top row) and 200 (bottom row). (C) Serum level of deoxypyridinole cross-links (DPD) and osteocalcin in WT, CD44$^{-/-}$, hTNFtg, and CD44$^{-/-}$ hTNFtg mice.

Absence of CD44 in bone marrow but not stromal cells is critical for the phenotype of CD44$^{-/-}$ hTNFtg mice

To distinguish whether deregulation of inflammatory bone destruction was due to lack of CD44 on stromal or bone marrow cells, we generated radiation chimeras of WT, CD44$^{-/-}$, and hTNFtg genotypes by bone marrow transplantation. hTNFtg mice challenged with hTNFtg bone marrow served as positive control and exhibited a progressive destructive arthritis (Fig. 6, A and B). However, when WT or CD44$^{-/-}$ mice were challenged with hTNFtg bone marrow, arthritis did not develop, indicating that overexpression of TNF by stromal but not bone marrow cells is critical for induction of arthritis (17). Transfer of WT bone marrow into hTNFtg mice, on the other hand, led to the development of a relatively mild arthritis. In contrast, when hTNFtg mice were challenged with CD44$^{-/-}$ bone marrow, severe arthritis ensued, which was significantly enhanced compared with arthritis after transfer of WT bone marrow cells to hTNFtg animals (Fig. 6, A and B). These data suggest that TNF overexpression by stromal cells together with CD44 deficiency of bone marrow cells is responsible for the severe inflammatory and destructive phenotype of CD44$^{-/-}$ hTNFtg mice.

Increased production of IL-1 and IL-6 and enhanced activation of p38 mitogen-activated protein kinase (MAPK) in osteoclasts of CD44$^{-/-}$ hTNFtg mice

To better define the increase in osteoclastogenesis and bone destruction in CD44$^{-/-}$ hTNFtg mice, cytokine production, osteoclastogenic signals, and intracellular signaling pathways of osteoclasts of the various genotypes were analyzed. Osteoclasts from CD44$^{-/-}$ hTNFtg mice showed significantly increased production of IL-1 and IL-6 compared with cells from hTNFtg mice. Moreover, increased levels of these two cytokines were observed in the serum of CD44$^{-/-}$ hTNFtg mice (Fig. 7 A). There was no difference between hTNFtg and CD44$^{-/-}$ hTNFtg mice in the levels of human TNF, murine TNF, and IL-4. Moreover, the balance of RANKL and its decoy receptor osteoprotegerin (OPG) was equal in hTNFtg and CD44$^{-/-}$ hTNFtg mice, as shown by almost identically elevated serum levels of RANKL and OPG in WT and CD44$^{-/-}$ mice (Fig. 7 B). In addition, surface expression of RANKL and M-CSF receptors, RANK and c-fms, respectively, did not differ among osteoclast precursors of hTNFtg and CD44$^{-/-}$ hTNFtg genotypes (Fig. 7 C). Next, we analyzed intracellular protein kinase activation in hTNFtg and CD44$^{-/-}$ hTNFtg os-

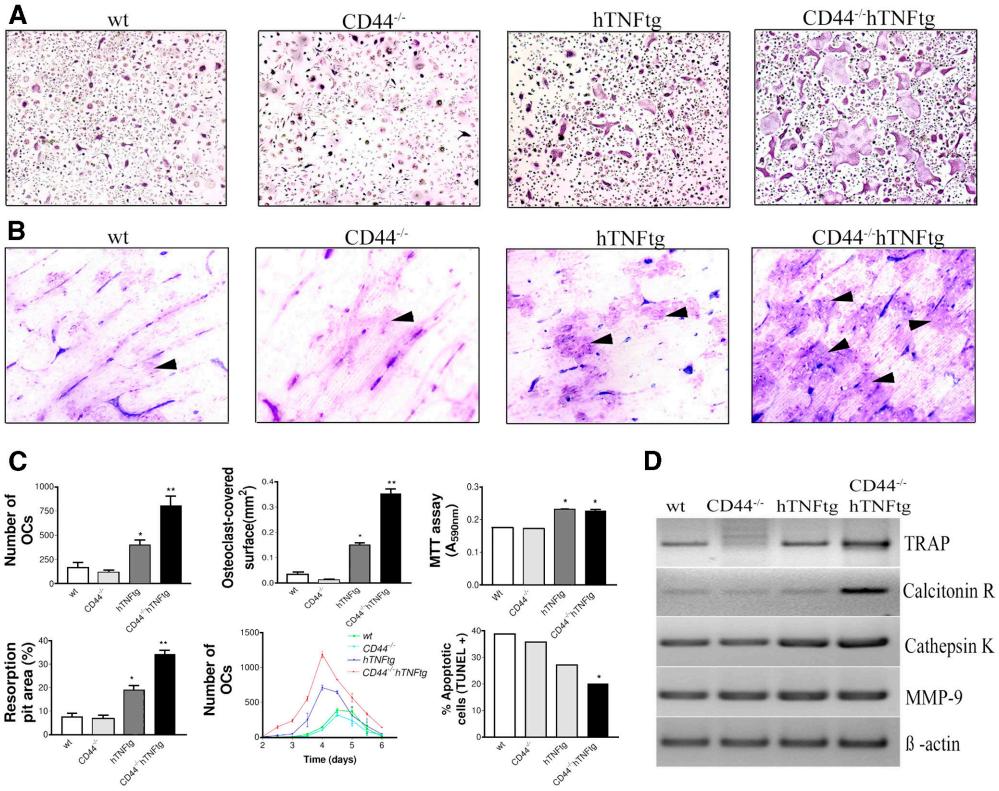

Figure 5. Ex vivo analysis of osteoclast formation. (A) Formation of TRAP$^+$ cells in the presence of M-CSF and RANKL in spleen cells from WT, CD44$^{-/-}$, hTNFtg, and CD44$^{-/-}$ hTNFtg mice. (B) Bone resorption assay showing formation of resorption pits (arrowheads). Original magnification of 100. (C) Quantitative analysis of number, size, and resorptive capacity of osteoclasts and time response curve of osteoclastogenesis. Apoptosis rate (TUNEL assay) and proliferation rate (MTT assay) of osteoclasts. Data are mean ± SD. Asterisks indicate significant ($P < 0.05$) difference. (D) RT-PCR for osteoclast markers from total RNA of cultivated osteoclasts of WT, CD44$^{-/-}$, hTNFtg, and CD44$^{-/-}$ hTNFtg mice.

teoclasts. Phosphorylation of p38 MAPK and to a lesser extent JNK was markedly increased in CD44$^{-/-}$ hTNFtg compared with hTNFtg osteoclasts upon stimulation with RANKL (Fig. 8 A), whereas activation of Akt, Erk, and IkB did not differ between hTNFtg and CD44$^{-/-}$ hTNFtg osteoclasts. Remarkably, the addition of RANKL resulted in an enhanced activation of p38 MAPK in osteoclasts of CD44$^{-/-}$ hTNFtg mice, which was not observed in hTNFtg mice. The addition of the p38 MAPK inhibitor SB203580 strongly inhibited osteoclastogenesis, emphasizing the central role of p38 MAPK signaling in osteoclast formation in CD44$^{-/-}$ hTNFtg mice (Fig. 8 B). This was further supported by immunohistochemical analyses in vivo, which demonstrated high expression of p38 MAPK in multinucleated osteoclasts of CD44$^{-/-}$ hTNFtg mice at sites of erosion fronts, which was more pronounced than in hTNFtg animals (Fig. 8 C).

Absence of CD44$^{-/-}$ leads to an increase in TNF responsiveness by enhanced p38 MAPK activation and a decrease of MAPK phosphatase (MKP)-1

In light of the excessive osteoclastogenesis in CD44$^{-/-}$ hTNFtg but not CD44$^{-/-}$ mice, we hypothesized that TNF may directly activate CD44$^{-/-}$ osteoclast precursors. This was supported by the observation that the osteoclastogenic capacity of RANKL was equal in WT and CD44$^{-/-}$ mice but dramatically different when TNF was present. Even low concentrations of RANKL, which did not induce osteoclastogenesis in hTNFtg precursors, were sufficient to induce osteoclasts in CD44$^{-/-}$ hTNFtg precursors (Fig. 9 A). Upon stimulation with TNF, in vitro osteoclast formation was significantly enhanced in cells derived from CD44$^{-/-}$ compared with WT mice (Fig. 9 A), indicating that the absence of CD44 leads to an increased TNF responsiveness of osteoclasts. Moreover, activation of p38 MAPK was more pronounced in cells from CD44$^{-/-}$ than WT mice upon stimulation with TNF, whereas it did not differ upon stimulation with RANKL (Fig. 9 B). Interestingly, analysis of p38 MAPK signaling molecules revealed identical activation of the upstream kinase MKK3/6 but diminished levels of the downstream phosphatase MKP-1 in cells from CD44$^{-/-}$ mice compared with WT mice (Fig. 9 B). Finally, to prove that the absence of CD44 sensitizes for inflammation-dependent osteoclast formation in vivo, we challenged WT and CD44$^{-/-}$ mice by subperiosteal injection of LPS into the calvarial bone. Administration of LPS led to formation of an inflammatory infiltrate as well as osteoclastogenesis. Measurement of osteoclast numbers in the calvarial

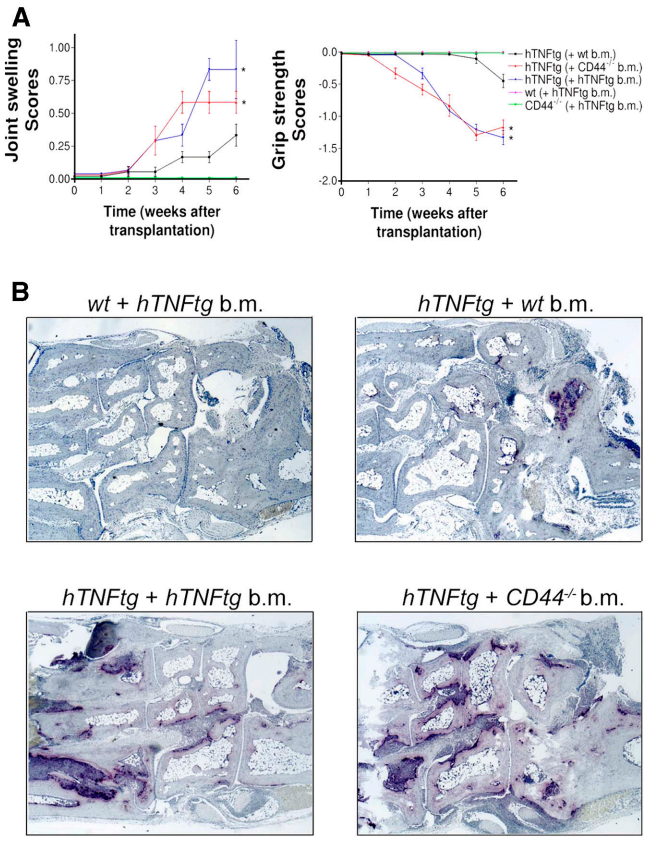

Figure 6. Development of arthritis in radiation chimeric mice. (A) Clinical assessment of arthritis by measurement of paw swelling and grip strength. (B) TRAP-stained histological sections showing inflammation and bone destruction in the tarsal region from the hind paws 6 wk after bone marrow transplantation. b.m., bone marrow. Original magnification of 250.

bone showed a significant threefold increase in $CD44^{-/-}$ mice compared with WT mice (Fig. 9 C).

DISCUSSION

Formation of osteoclasts and consequent joint destruction is a hallmark of RA. Synovial osteoclast formation is based on the influx of mononuclear osteoclast precursors into the joint as well as the articular expression of molecules, such as M-CSF, RANKL, and TNF, which support osteoclastogenesis (7, 18–21). Even long-standing and highly active arthritis does not cause joint destruction if osteoclasts are absent (8, 9). Formation of osteoclasts, however, is a complex process, which requires fusion of up to 20 single cells and therefore depends on the disruption of complex cell–matrix interactions.

CD44 is a type I transmembrane glycoprotein that is expressed on most cell types and interacts with several different extracellular matrix components, such as hyaluronic acid (10, 22). CD44 plays a major role in the maintenance of tissue integrity. Interestingly, under physiological conditions deficiency of CD44 results in no major disease phenotype (11). However, recent studies, which addressed a potential role of CD44 in models of acute inflammatory reactions in lung and liver, have shown that deficiency of CD44 leads to a profoundly more aggressive and prolonged course of disease (23–25.) This was due to altered function of granulocytes, showing accelerated migration and impaired clearance as well as impaired lymphocyte apoptosis, respectively. On the other hand, autoimmune conditions such as collagen-induced arthritis occur with lower frequency and severity in animals in which CD44 has been blocked pharmacologically or has been deleted genetically (26–29). The role of CD44 in chronic inflammatory disease, which is based on persistent up-regulation of proinflammatory mediators and is associated with profound tissue remodeling such as local and systemic bone loss, is yet unknown.

Until now, a direct role of CD44 in osteoclasts has only been addressed by in vitro studies. Thus, engagement of CD44 with matrix ligands or antibodies mimicking matrix ligands suppressed osteoclast formation (27, 28). This mechanism, however, does not appear to be critical in physiological conditions, because $CD44^{-/-}$ mice showed no signs of increased bone resorption in vitro or in vivo. However, under conditions of chronic inflammation, CD44 emerged as a critical determinant of osteoclastogenesis. TNF triggered a far more potent osteoclastogenic response if osteoclast precursors were CD44 deficient. This was manifested by an excess of osteoclast formation and generation of giant osteoclasts, which enabled rapid bone resorption and accelerated joint destruction and osteopenia. The mechanism appeared to depend on a higher sensitivity of CD44-deficient osteoclast precursors toward TNF and indicates that osteoclastogenesis is deregulated in vitro and in vivo when matrix molecules fail to interact with monocytes via CD44. This increased sensitivity resulted from an enhanced signaling through the p38 MAPK pathway, an essential step during osteoclastogenesis (30–32), and lead to increased production of TNF-dependent cytokines, such as IL-1 and IL-6. Both of them are important for osteoclastogenesis and their induction by TNF depends on activation of p38 MAPK (33–36). The increased sensitivity of $CD44^{-/-}$ mice for TNF-mediated bone loss is further corroborated by the observation that LPS, which activates the proinflammatory cytokine cascade, induced enhanced osteoclastogenesis when injected subperiosteally into $CD44^{-/-}$ mice.

CD44 appears to influence molecules upstream of p38 MAPK. MKP-1 is known as an important negative regulator of p38 MAPK (37). In fact, deficiency in CD44 appears to down-regulate the downstream phosphatase MKP-1 rather than increase the activity of the upstream kinases MKK3 and MKK6. This suggests that extracellular matrix interaction via CD44 may prevent excessive osteoclast differentiation through its regulatory role on the p38 MAPK pathway. Whether increased p38 MAPK signaling also affects the function of mature osteoclasts is less clear. Increased activation of p38 MAPK has been found in osteoclasts of $CD44^{-/-}$ hTNFtg mice in vivo. Moreover, the fact that osteoclast size was increased in $CD44^{-/-}$ hTNFtg mice in vitro and in vivo and

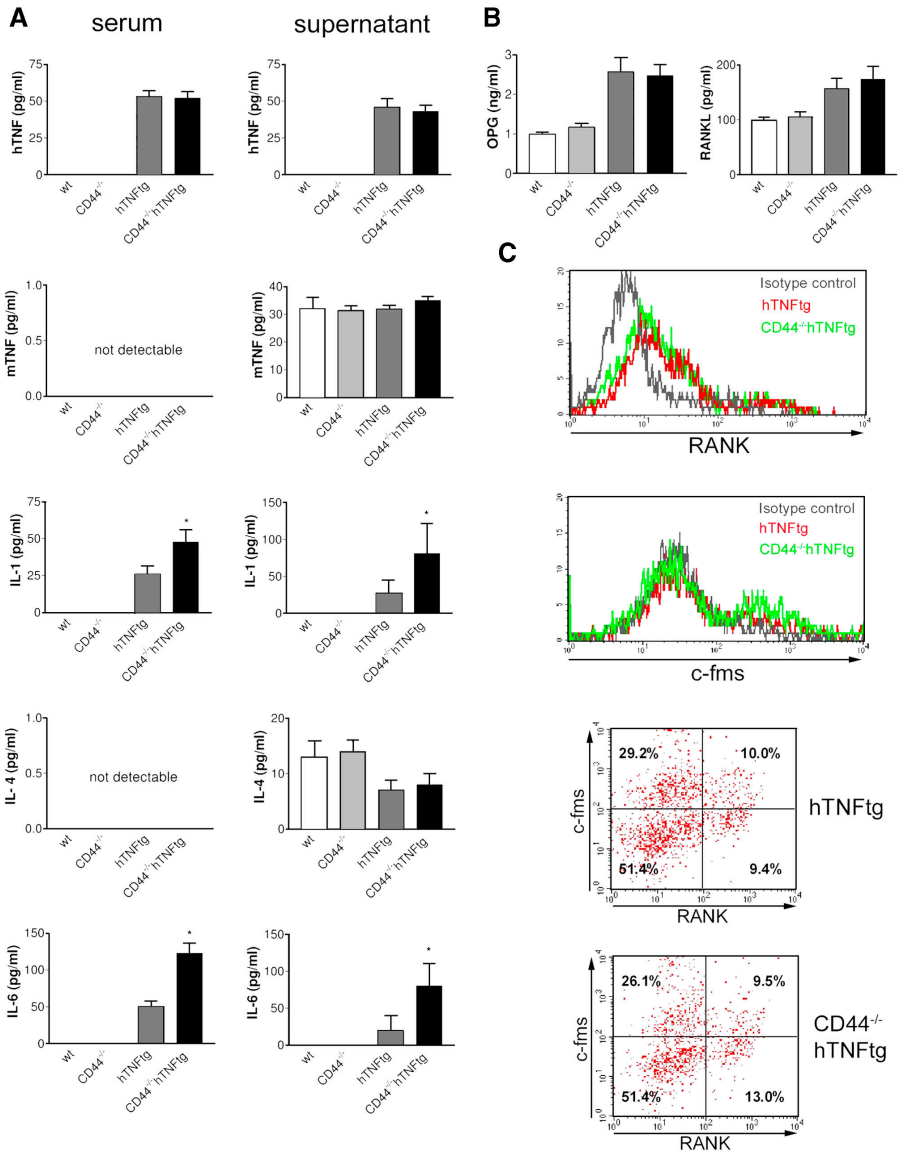

Figure 7. Cytokine production, bone markers, and surface receptor expression. (A) Cytokine levels of hTNF, murine TNF (mTNF), IL-1, IL-4, and IL-6 in sera (left) and supernatants (right) from osteoclast cultures isolated from WT, CD44$^{-/-}$, hTNFtg, and CD44$^{-/-}$ hTNFtg mice. (B) Serum levels of RANKL and OPG in the aforementioned genotypes. (C) FACS analysis of surface expression of RANK (by RANKL-FITC) and c-fms (by quantum red-labeled anti–c-fms antibody) on osteoclast precursors from hTNFtg and CD44$^{-/-}$ hTNFtg mice.

that the rate of apoptosis was low in CD44$^{-/-}$ hTNFtg osteoclasts supports this argument. In fact, the life span of osteoclasts and their susceptibility to apoptotic cell death is known as a critical parameter for the size of osteoclasts (36). Thus, excessive p38 MAPK activity induced by TNF may also increase the survival of osteoclasts in the absence of CD44.

These data also suggest that the interaction of osteopontin with CD44 is not critical for osteoclastogenesis. Osteopontin is a phosphorylated glycoprotein, which is expressed at sites of inflammation and binds to a variety of cell surface receptors, preferentially integrins and CD44 (13). The role of osteopontin in autoimmune conditions is rather conflicting. Mitigation of experimental autoimmune encephalomyelitis and collagen-induced arthritis have been reported in the absence of osteopontin, although the latter finding is controversial and has not been observed by others (38–41). Moreover, the serum transfer model of arthritis is not altered by the absence of osteopontin (39). From these data, it is evident, however, that the interaction of osteopontin with CD44 is not a relevant factor for arthritic bone erosion. It is unclear whether its interaction with other receptors such as αvβ3 integrin is important, despite the fact that osteopontin expression in synovial tissue and osteopontin serum levels were not altered by the absence of CD44 (not depicted).

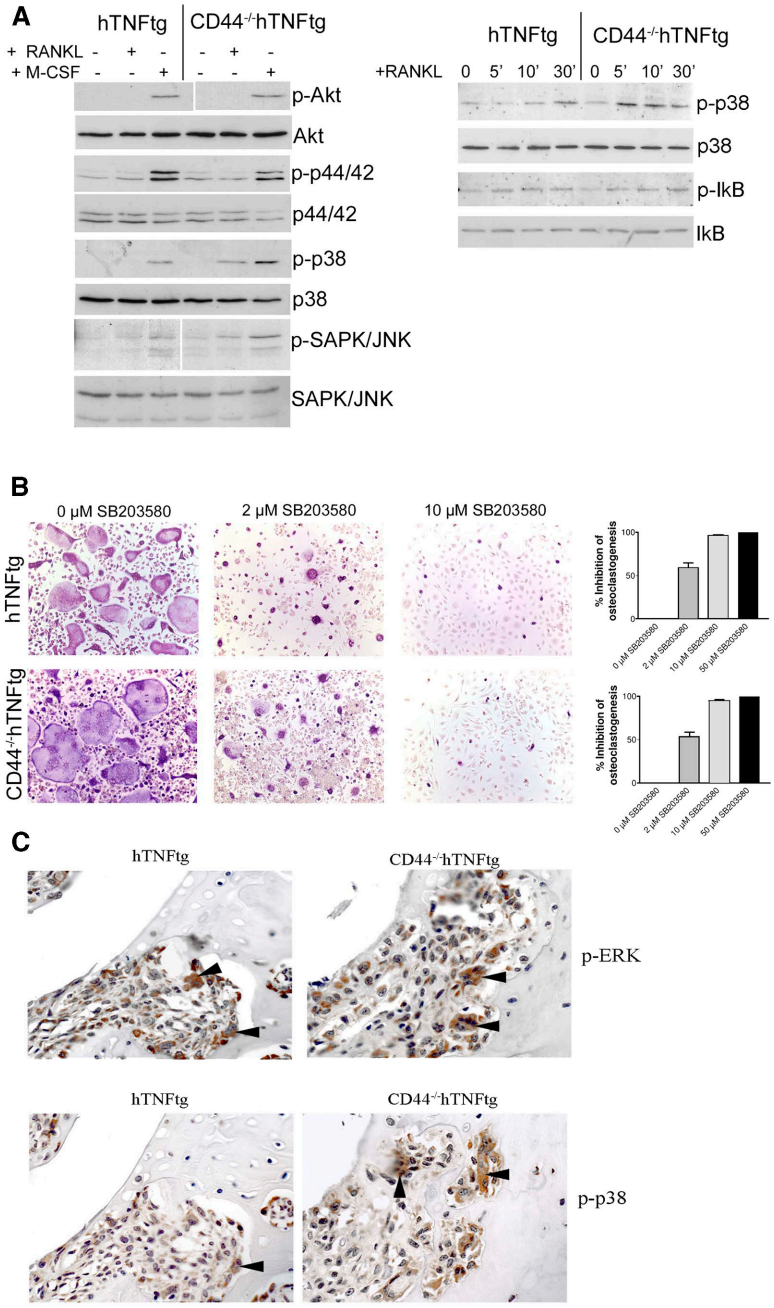

Figure 8. Activation of intracellular signaling pathways. (A) Analysis of intracellular protein kinase activation in osteoclasts from hTNFtg and CD44$^{-/-}$ hTNFtg mice upon stimulation with RANKL and M-CSF. (B) Inhibition of osteoclastogenesis by p38 MAPK inhibitor SB 203580 evaluated by TRAP staining. (C) Immunohistochemical analysis of p38 MAPK and ERK phosphorylation in synovial osteoclasts of hTNFtg and CD44$^{-/-}$ hTNFtg mice in vivo (brown, arrows). Original magnification of 400.

Absence of CD44 on monocytes and overexpression of TNF by stromal cells was found to be essential for the observed dramatic deregulation of osteoclast-mediated bone resorption in CD44-deficient hTNFtg mice, whereas absence of CD44 on stromal cells and overexpression of TNF on bone marrow cells did not cause any bone phenotype nor arthritis. This indicates that in this disease model two mechanisms are essentially involved in inflammatory bone destruction: (a) Neighboring stromal cells need to provide excess amounts of proinflammatory factors, such as TNF, which induce osteoclast differentiation from mononuclear precursors; and (b) Osteoclastogenesis must overcome CD44-mediated cell–matrix interactions, which prevent tissue remodeling and damage. In fact, this

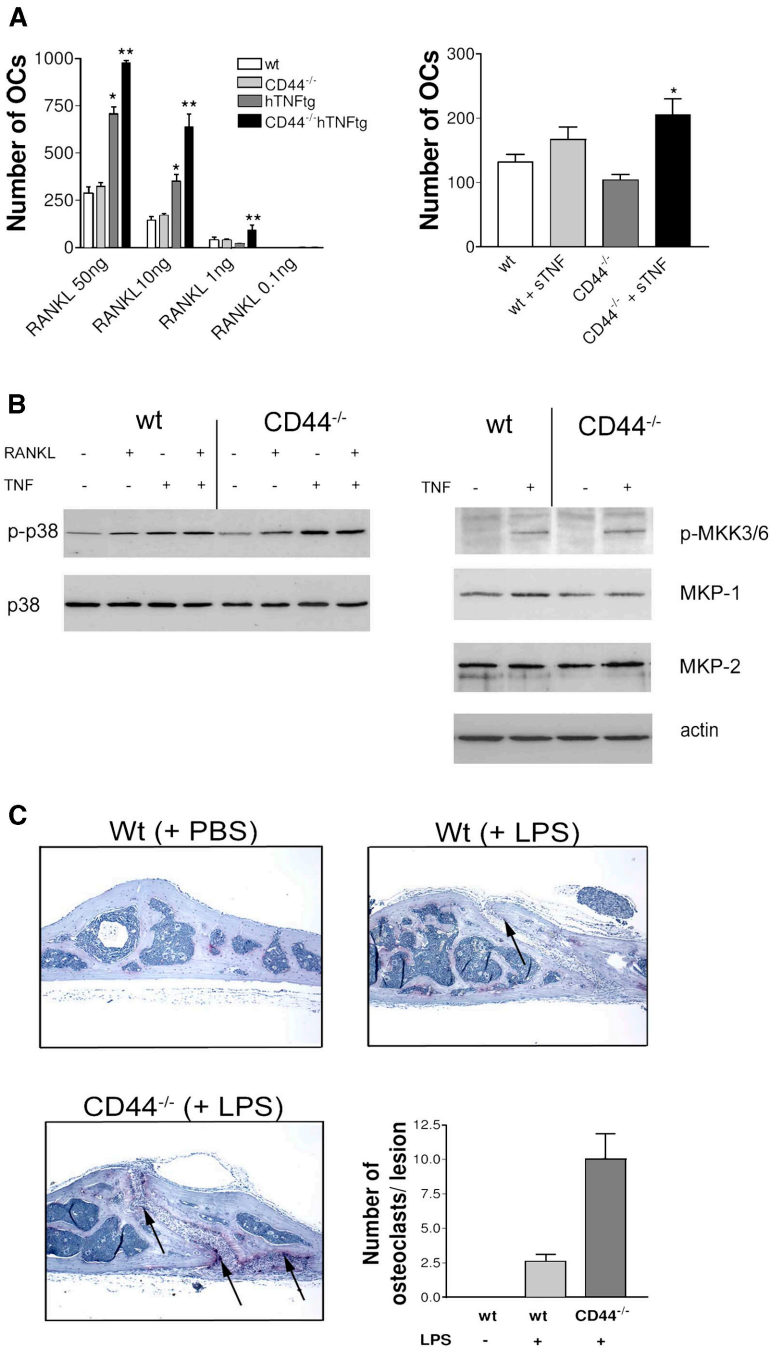

Figure 9. Osteoclastogenic effects of TNF in the absence of CD44. (A) Dose response analysis of RANKL on osteoclast differentiation in WT, CD44$^{-/-}$, hTNFtg, and CD44$^{-/-}$ hTNFtg mice (left). Effect of exogenous TNF on the formation of osteoclasts in WT and CD44$^{-/-}$ mice (right). (B) Analysis of MAPK activation upon stimulation with RANKL, TNF, or both in osteoclasts from WT and CD44$^{-/-}$ mice (left). Assessment of upstream kinase activation and protein phosphatases after stimulation with TNF in osteoclasts from WT and CD44$^{-/-}$ mice. (C) Analysis of osteoclast formation by TRAP staining (purple, arrows) upon subperiosteal injection of LPS (or PBS) in the calvariae of WT and CD44$^{-/-}$ mice. Original magnification of 50.

latter regulatory mechanism appears to be highly important during chronic overexpression of proinflammatory cytokines as implied by the severity of bone loss found in CD44$^{-/-}$ hTNFtg mice. This is additionally supported by observations that TNF stimulates the interaction of hyaluronic acid with CD44, indicating that TNF itself induces regulatory cell–matrix interaction. Strengthening of cell–matrix interactions through CD44 may thus provide a novel therapeutic principle to counteract tissue damage due to inflammation.

MATERIALS AND METHODS

Animals. Tg197 human TNF transgenic mice (hTNFtg; genetic background C57BL6; reference 14) and CD44$^{-/-}$ mice (genetic background: C57BL6; reference 11) were crossed, and F2 generations were identified by PCR from tail DNA using the following primers: hTNF transgene construct: 5′-TACCCCCTCCTTCAGACACC-3′ and 5′-GCCCTTCATAATATCCCCCA-3′; CD44 WT: 5′-GGCGACTAGATCCCTCCGTT-3′ and 5′-ACCCAGAGGCATACCAGCTG-3′; and CD44 knockout: 5′-GTTTCATCCAGCACGCCAT-3′ and 5′-ATTCAGGCTGCGCAACTGT-3′. All data were generated from littermates. Animals were killed by cervical dislocation 10 wk after birth. All animal procedures were approved by the local ethical committee.

Clinical assessment. Paw swelling was assessed in all four paws by using a semiquantitative score as described previously (8): 0, no swelling; 1, mild swelling of toes and ankle; 2, moderate swelling of toes and ankle; 3, severe swelling of toes and ankle. Grip strength (8) was similarly assessed: 0, normal grip strength; −1, mildly reduced grip strength; −2, severely reduced grip strength; −3 no grip at all. Assessments were performed in blinded fashion between weeks 4 and 10 of age.

Histological analyses. 2-μm decalcified paraffin-embedded sections were stained with hematoxylin and eosin, toluidine blue, and TRAP (Leukocyte Phosphatase Staining Kit; Sigma Diagnostics). For immunohistochemical analyses, sections were incubated with anti-CD44 rat polyclonal antibody (IM-7 clone; BD Biosciences), anti–phospho-p38 MAPK, anti–phospho-ERK, anti–phospho-JNK monoclonal antibodies (all from Santa Cruz Biotechnology, Inc.), or biotinylated hyaluronic acid binding protein (Seikagaku).

Micro-CT analysis and histomorphometry. Micro-CT was performed on vertebrae and long bones using MICRO-CT20 equipment (SCANCO-Medical). For histomorphometry, tibiae were embedded in methacrylate (Echnovit; Heraeus Kulzer) and 3–4-μm sections were stained with von Kossa and toluidine blue. Histomorphometry of metaphyses was performed using an Axioskop 2 microscope (Carl Zeiss MicroImaging, Inc.) and OsteoMeasure Analysis System (OsteoMetrics) according to international standards (15, 42).

Ex vivo osteoclastogenesis and bone resorption assay. CD11b^{+} mononuclear cells (>90% purity) were isolated from the spleen and cultured in 10% FCS/DMEM supplemented with 30 ng/ml M-CSF and 50 ng/ml RANKL (both from R&D Systems). Inhibition of osteoclastogenesis was performed in the presence of 0, 2, 10, and 50 μM of p38 MAPK inhibitor SB 203580 (Calbiochem). Osteoclasts were detected by the presence of TRAP enzyme activity. Bone resorption assay was performed on 0.4-mm thick bovine bone slices. Areas of bone resorption were planimetrically analyzed using the Axioskop 2 microscope (Carl Zeiss MicroImaging, Inc.) and the OsteoMeasure Analysis System (OsteoMetrics).

RT-PCR. Total RNA was isolated from cultivated osteoclasts using the RNeasy Mini kit (QIAGEN). 1 μg total RNA was used for first strand cDNA synthesis (Amersham Biosciences) and 1 μl cDNA was then used for PCR using the following primers: cathepsin K: 5′-GGAAGAAGACTCACCAGAAGC-3′ and 5′-GTCATATAGCCGCCTCCACAG-3′; MMP-9: 5′-CCTGTGTGTTCCCGTTCATCT-3′ and 5′-CGCTGGAATGATCTAAGCCCA-3′; TRAP: 5′-ACAGCCCCCACTCCCACCCT-3′ and 5′-TCAGGGTCTGGGTCTCCTTGG-3′; calcitonin receptor: 5′-CATTCCTGTACTTGGTTGGC-3′ and 5′-AGCAATCGACAAGGAGTGAC-3′; and β-actin: 5′-TGTGATGGTGGGAATGGGTCAG-3′ and 5′-TTTGATGTCACGCACGATTTCC-3′.

Analysis of protein kinase activation. CD11b^{+} mononuclear cells (>90% purity) were isolated from the spleen and cultured in 10% FCS/DMEM supplemented with 30 ng/ml M-CSF and 50 ng/ml RANKL (both from R&D Systems). Cultured osteoclasts were starved in serum-free DMEM for 2 h on day 3 and stimulated with 50 ng/ml RANKL or 30 ng/ml M-CSF or 10 ng/ml TNF (Strathmann Biotec AG) or DMEM alone for 5, 10, 30, or only 15 min. Cells were lysed in buffer containing 10 mM Tris, pH 7.4, 150 mM NaCl, 1 mM EDTA, 0.2% sodium deoxycholate, 1% NP-40, 1 mM NaF, 2 mM Na_3VO_4, and protease inhibitors. Western blotting was performed with polyclonal antibodies against the phosphorylated forms of the protein kinases Akt, p38 MAPK, ERK (p44/42 MAP kinase), SAPK/JNK, IkB and MKK3/MKK6 (all antibodies from Cell Signaling), and for MKP-1 and MKP-2 (both from Santa Cruz Biotechnology, Inc.). For the purposes of control, total Akt, p38 MAPK, ERK, SAPK/JNK, IkB (all from Cell Signaling), and actin (Sigma-Aldrich) were also stained.

Apoptosis and proliferation assay. The apoptosis rate of cultured osteoclasts was measured by TUNEL assay using an In Situ Cell Death Detection Kit (Roche). The proliferation rate of osteoclasts was examined using an MTT (3-[4,5-dimethylthiazol-2-yl]-2,5-diphenyl tetrazolium bromid) assay (Cell Proliferation Kit I; Roche).

FACS analysis. Isolated splenocytes and bone marrow cells from tibiae and femurs were cultured in DMEM with 30 ng/ml M-CSF for 1–2 d. Cells were then stained with RANKL-FITC and biotinylated antibody against c-fms (both provided by J. Penninger, IMBA, Vienna, Austria) using standard FACS procedures.

Generation of radiation chimeras. 4-wk-old female recipient mice received a whole body irradiation of 10 Gy and were then challenged with 5×10^6 bone marrow cells into the tail vein. Bone marrow cells were isolated from long bones of age- and sex-matched donor mice and washed in M199 medium (Sigma-Aldrich) supplemented with 10 mM Hepes buffer (ICN Biomedicals), 10 ng/ml DNase, and 4 ng/ml gentamycin (both from Sigma-Aldrich). Mice were weekly assessed for clinical signs of arthritis and killed 6 wk after bone marrow transplantation.

Measurement of cytokines and serum parameters of bone metabolism. Levels of hTNF, murine TNF (mTNF), IL-1 (mIL-1), mIL-4, mIL-6, soluble RANKL, and OPG in mouse sera and/or in supernatants of osteoclast cultures were performed by ELISA according to the manufacturer's recommendations (all from R&D Systems). Desoxypyridinolin cross-links were measured by enzyme immunoassay (Quidel) after previous hydrolysis of serum samples according to the manufacturer's recommendations. Osteocalcin was measured by immunoradiometric assay (Immutopics).

Subperiosteal injection of LPS. WT ($n = 5$) and CD44$^{-/-}$ mice ($n = 5$) were anesthetized and received 100 μl subperiosteal injection of 500 μg LPS (Sigma-Aldrich) or PBS. Animals were killed 5 d later and calvariae were fixed in 4.5% formaldehyde for 5 h and were then decalcified in 14% EDTA (pH adjusted to 7.2 by the addition of 25% ammonia solution; Merck) at 4°C for 5 d. Osteoclast numbers were analyzed after TRAP staining of paraffin-embedded sections.

Statistical analysis. Data are given as mean ± SEM. Group mean values were compared by using the unpaired two-tailed Student's *t* test.

We thank Birgit Türk and Margarete Tryniecki for excellent technical assistance.

This study was supported by the START price of the Austrian Science Fund (to G. Schett) and the Center of Molecular Medicine of the Austrian Academy of Sciences (CeMM), Vienna, Austria (to S. Hayer, G. Steiner, J.S. Smolen, and G. Schett).

The authors have no conflicting financial interests.

Submitted: 29 April 2004
Accepted: 4 January 2005

REFERENCES

1. Smolen, J.S., and G. Steiner. 2003. Therapeutic strategies for rheumatoid arthritis. *Nat. Rev. Drug Discov.* 2:473–488.
2. Firestein, G.S. 2003. Evolving concepts of rheumatoid arthritis. *Nature.* 423:356–361.

3. Woolf, A.D. 1991. Osteoporosis in rheumatoid arthritis–the clinical viewpoint. *Br. J. Rheumatol.* 30:82–84.
4. Peel, N.F., R. Eastell, and R.G. Russell. 1991. Osteoporosis in rheumatoid arthritis–the laboratory perspective. *Br. J. Rheumatol.* 30:84–85.
5. Scott, D.L., K. Pugner, K. Kaarela, D.V. Doyle, A. Woolf, J. Holmes, and K. Hieke. 2000. The links between joint damage and disability in rheumatoid arthritis. *Rheumatology (Oxford).* 39:122–132.
6. Gravallese, E.M., Y. Harada, J.T. Wang, A.H. Gorn, T.S. Thornhill, and S.R. Goldring. 1998. Identification of cell types responsible for bone resorption in rheumatoid arthritis and juvenile rheumatoid arthritis. *Am. J. Pathol.* 152:943–951.
7. Gravallese, E.M., C. Manning, A. Tsay, A. Naito, C. Pan, E. Amento, and S.R. Goldring. 2000. Synovial tissue in rheumatoid arthritis is a source of osteoclast differentiation factor. *Arthritis Rheum.* 43:250–258.
8. Redlich, K., S. Hayer, R. Ricci, J.P. David, M. Tohidast-Akrad, G. Kollias, G. Steiner, J.S. Smolen, E.F. Wagner, and G. Schett. 2002. Osteoclasts are essential for TNF-alpha-mediated joint destruction. *J. Clin. Invest.* 110:1419–1427.
9. Pettit, A.R., H. Ji, D. von Stechow, R. Muller, S.R. Goldring, Y. Choi, C. Benoist, and E.M. Gravallese. 2001. TRANCE/RANKL knockout mice are protected from bone erosion in a serum transfer model of arthritis. *Am. J. Pathol.* 159:1689–1699.
10. Lesley, J., R. Hyman, and P.W. Kincade. 1993. CD44 and its interaction with extracellular matrix. *Adv. Immunol.* 54:271–335.
11. Protin, U., T. Schweighoffer, W. Jochum, and F. Hilberg. 1999. CD44-deficient mice develop normally with changes in subpopulations and recirculation of lymphocyte subsets. *J. Immunol.* 163:4917–4923.
12. Aruffo, A., I. Stamenkovic, M. Melnick, C.B. Underhill, and B. Seed. 1990. CD44 is the principal cell surface receptor for hyaluronate. *Cell.* 61:1303–1313.
13. Weber, G.F., S. Ashkar, M.J. Glimcher, and H. Cantor. 1996. Receptor-ligand interaction between CD44 and osteopontin (Eta-1). *Science.* 271:509–512.
14. Keffer, J., L. Probert, H. Cazlaris, S. Georgopoulos, E. Kaslaris, D. Kioussis, and G. Kollias. 1991. Transgenic mice expressing human tumour necrosis factor: a predictive genetic model of arthritis. *EMBO J.* 10:4025–4031.
15. Schett, G., K. Redlich, S. Hayer, J. Zwerina, B. Bolon, C. Dunstan, B. Gortz, A. Schulz, H. Bergmeister, G. Kollias, et al. 2003. Osteoprotegerin protects against generalized bone loss in tumor necrosis factor-transgenic mice. *Arthritis Rheum.* 48:2042–2051.
16. Redlich, K., B. Gortz, S. Hayer, J. Zwerina, N. Doerr, P. Kostenuik, H. Bergmeister, G. Kollias, G. Steiner, J.S. Smolen, and G. Schett. 2004. Repair of local bone erosions and reversal of systemic bone loss upon therapy with anti-tumor necrosis factor in combination with osteoprotegerin or parathyroid hormone in tumor necrosis factor-mediated arthritis. *Am. J. Pathol.* 164:543–555.
17. Aidinis, V., D. Plows, S. Haralambous, M. Armaka, P. Papadopoulos, M.Z. Kanaki, D. Koczan, H.J. Thiesen, and G. Kollias. 2003. Functional analysis of an arthritogenic synovial fibroblast. *Arthritis Res. Ther.* 5:R140–R157.
18. Romas, E., M.T. Gillespie, and T.J. Martin. 2002. Involvement of receptor activator of NFkappaB ligand and tumor necrosis factor-alpha in bone destruction in rheumatoid arthritis. *Bone.* 30:340–346.
19. Teitelbaum, S.L. 2000. Bone resorption by osteoclasts. *Science.* 289: 1504–1508.
20. Seitz, M., P. Loetscher, M.F. Fey, and A. Tobler. 1994. Constitutive mRNA and protein production of macrophage colony-stimulating factor but not of other cytokines by synovial fibroblasts from rheumatoid arthritis and osteoarthritis patients. *Br. J. Rheumatol.* 33:613–619.
21. Chu, C.Q., M. Field, M. Feldmann, and R.N. Maini. 1991. Localization of tumor necrosis factor alpha in synovial tissues and at the cartilage-pannus junction in patients with rheumatoid arthritis. *Arthritis Rheum.* 34:1125–1132.
22. Ponta, H., L. Sherman, and P.A. Herrlich. 2003. CD44: from adhesion molecules to signalling regulators. *Nat. Rev. Mol. Cell Biol.* 4:33–45.
23. Teder, P., R.W. Vandivier, D. Jiang, J. Liang, L. Cohn, E. Pure, P.M. Henson, and P.W. Noble. 2002. Resolution of lung inflammation by CD44. *Science.* 296:155–158.
24. Chen, D., R.J. McKallip, A. Zeytun, Y. Do, C. Lombard, J.L. Robertson, T.W. Mak, P.S. Nagarkatti, and M. Nagarkatti. 2001. CD44-deficient mice exhibit enhanced hepatitis after concanavalin A injection: evidence for involvement of CD44 in activation-induced cell death. *J. Immunol.* 166:5889–5897.
25. Schmits, R., J. Filmus, N. Gerwin, G. Senaldi, F. Kiefer, T. Kundig, A. Wakeham, A. Shahinian, C. Catzavelos, J. Rak, et al. 1997. CD44 regulates hematopoietic progenitor distribution, granuloma formation, and tumorigenicity. *Blood.* 90:2217–2233.
26. Stoop, R., H. Kotani, J.D. McNeish, I.G. Otterness, and K. Mikecz. 2001. Increased resistance to collagen-induced arthritis in CD44-deficient DBA/1 mice. *Arthritis Rheum.* 44:2922–2931.
27. Kania, J.R., T. Kehat-Stadler, and S.R. Kupfer. 1997. CD44 antibodies inhibit osteoclast formation. *J. Bone Miner. Res.* 12:1155–1164.
28. Sterling, H., C. Saginario, and A. Vignery. 1998. CD44 occupancy prevents macrophage multinucleation. *J. Cell Biol.* 143:837–847.
29. Mikecz, K., K. Dennis, M. Shi, and J.H. Kim. 1999. Modulation of hyaluronan receptor (CD44) function in vivo in a murine model of rheumatoid arthritis. *Arthritis Rheum.* 42:659–668.
30. Matsumoto, M., T. Sudo, T. Saito, H. Osada, and M. Tsujimoto. 2000. Involvement of p38 mitogen-activated protein kinase signaling pathway in osteoclastogenesis mediated by receptor activator of NF-kappa B ligand (RANKL). *J. Biol. Chem.* 275:31155–31161.
31. Li, X., N. Udagawa, K. Itoh, K. Suda, Y. Murase, T. Nishihara, T. Suda, and N. Takahashi. 2002. p38 MAPK-mediated signals are required for inducing osteoclast differentiation but not for osteoclast function. *Endocrinology.* 143:3105–3113.
32. Li, X., N. Udagawa, M. Takami, N. Sato, Y. Kobayashi, and N. Takahashi. 2003. p38 Mitogen-activated protein kinase is crucially involved in osteoclast differentiation but not in cytokine production, phagocytosis, or dendritic cell differentiation of bone marrow macrophages. *Endocrinology.* 144:4999–5005.
33. De Cesaris, P., D. Starace, A. Riccioli, F. Padula, A. Filippini, and E. Ziparo. 1998. Tumor necrosis factor-alpha induces interleukin-6 production and integrin ligand expression by distinct transduction pathways. *J. Biol. Chem.* 273:7566–7571.
34. Beyaert, R., A. Cuenda, W. Vanden Berghe, S. Plaisance, J.C. Lee, G. Haegeman, P. Cohen, and W. Fiers. 1996. The p38/RK mitogen-activated protein kinase pathway regulates interleukin-6 synthesis response to tumor necrosis factor. *EMBO J.* 15:1914–1923.
35. Baldassare, J.J., Y. Bi, and C.J. Bellone. 1999. The role of p38 mitogen-activated protein kinase in IL-1 beta transcription. *J. Immunol.* 162:5367–5373.
36. Takeshita, S., N. Namba, J.J. Zhao, Y. Jiang, H.K. Genant, M.J. Silva, M.D. Brodt, C.D. Helgason, J. Kalesnikoff, M.J. Rauh, et al. 2002. SHIP-deficient mice are severely osteoporotic due to increased numbers of hyper-resorptive osteoclasts. *Nat. Med.* 8:943–949.
37. Chen, P., J. Li, J. Barnes, G.C. Kokkonen, J.C. Lee, and Y. Liu. 2002. Restraint of proinflammatory cytokine biosynthesis by mitogen-activated protein kinase phosphatase-1 in lipopolysaccharide-stimulated macrophages. *J. Immunol.* 169:6408–6416.
38. Jansson, M., V. Panoutsakopoulou, J. Baker, L. Klein, and H. Cantor. 2002. Cutting edge: attenuated experimental autoimmune encephalomyelitis in eta-1/osteopontin-deficient mice. *J. Immunol.* 168:2096–2099.
39. Jacobs, J.P., A.R. Pettit, M.L. Shinohara, M. Jansson, H. Cantor, E.M. Gravallese, D. Mathis, and C. and Benoist. 2004. Lack of requirement of osteopontin for inflammation, bone erosion, and cartilage damage in the K/BxN model of autoantibody-mediated arthritis. *Arthritis Rheum.* 50:2685–2694.
40. Gravallese, E.M. 2003. Osteopontin: a bridge between bone and the immune system. *J. Clin. Invest.* 112:147–149.
41. Blom, T., A. Franzen, D. Heinegard, and R. Holmdahl. 2003. Comment on "The influence of the proinflammatory cytokine, osteopontin, on autoimmune demyelinating disease." *Science.* 299:1845.
42. Parfitt, A.M., M.K. Drezner, F.H. Glorieux, J.A. Kanis, H. Malluche, P.J. Meunier, S.M. Ott, and R.R. Recker. 1987. Bone histomorphometry: standardization of nomenclature, symbols, and units. Report of the ASBMR Histomorphometry Nomenclature Committee. *J. Bone Miner. Res.* 2:595–610.